Pramāṇa, Vol. 24, Nos 1 & 2, January & February 1985, pp. 397–421. © Printed in India.

Irradiation behaviour of nuclear fuels

P R ROY and D N SAH
Radiometallurgy Division, Bhabha Atomic Research Centre, Trombay, Bombay 400 085, India

Abstract. This paper gives a brief review of the important phenomena observed in metallic uranium and ceramic nuclear fuels during irradiation in reactors. The mechanism of irradiation growth, irradiation creep and swelling which are responsible for the dimensional instability of uranium has been described. Important phenomena observed in ceramic nuclear fuels, *e.g.* fuel densification, fuel restructuring, plutonium segregation, oxygen and fission product migration, irradiation creep, fission gas release and swelling have been discussed. A brief note is included on computer modelling for prediction of fuel element irradiation behaviour.

Keywords. Irradiation effects; nuclear fuels; metallic fuels; ceramic fuels; irradiation behaviour; irradiation growth; irradiation creep; swelling; densification; restructuring; fission gas release; fuel modelling.

PACS No. 28·40; 28·90

1. Introduction

Nuclear fuels are exposed to a unique and very severe thermal and radiation environment during their use in reactors. The behaviour of the fuel material in this environment is quite different from its behaviour outside the reactor. It is governed by the complex interplay of a large number of interactive physical, chemical, mechanical and metallurgical processes which become operative in the fuel in the reactor environment. A great deal of studies have been made and are still continuing to understand the irradiation behaviour of fuels in nuclear reactors. These studies have revealed spectacular changes in the geometry, dimensions, composition and microstructure of the fuels during and after fission due to irradiation. In this paper some of the important phenomena observed in two types of nuclear fuels *viz* metallic uranium fuels and ceramic fuels (oxide, mixed oxide and mixed carbide), which are relevant to India's nuclear programme, are described. As oxides are now the most widely used fuels in the present-day nuclear power reactors, they have been discussed at length. The paper briefly reviews the important findings about these phenomena and their mechanisms.

2. Irradiation damage in solid nuclear fuels

The radiation environment in the nuclear reactor core consists of fission fragments, high energy neutrons, charged particles and other radiations. The main source of radiation damage in nuclear fuels is the highly ionised fission fragments carrying a total of 165 MeV energy and the fast neutrons which have an energy upto 10 MeV. Fission

fragments and neutrons move rapidly through the lattice, exchanging their energy with the lattice atoms until they come to rest. The damage to the fuel by fission fragments is caused in the following three ways:

(i) *Fission spikes*: Each fission fragment is highly ionised (about 20+) and has a range of 6–10 microns in the fuel matrix. Over this small distance, the fission fragment releases all its energy which has an effect of raising the fuel temperature to more than 3000°C for a brief period of 10^{-11} seconds. This zone is called a fission spike. It is a cylindrical region of about 100 Å in radius with the fission fragment track as its axis. The end portion of the fission spike where the fission fragment comes to rest is characterised by severe disarrangement of lattice atoms and is often called displacement spike while the rest is called thermal spike (figure 1). Once the fission fragments come to rest, they are more usually described as fission products.

(ii) *Lattice defects*: Collision of fission fragments with lattice atoms of the fuel matrix produces primary knock-on atoms which have sufficient energy to displace other atoms from the fuel lattice. This gives rise to creation of several types of point defects in the lattice (figure 2). The formation of lattice defects in the fuel matrix provides the impetus for atomic diffusion of various species. All diffusion-controlled processes are enhanced

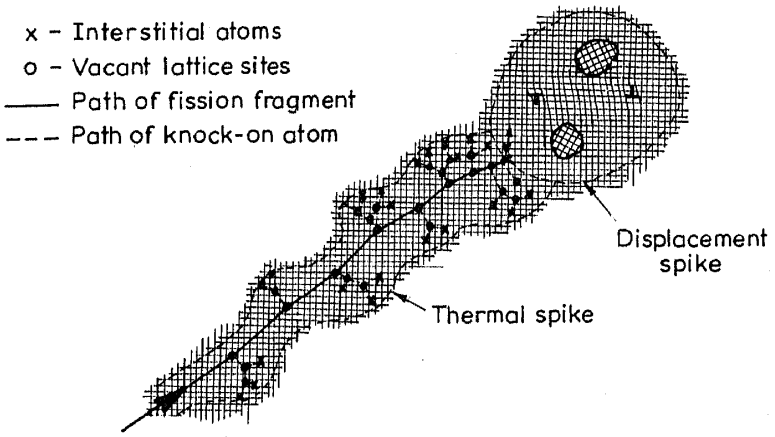

Figure 1. Schematic representation of the fission spike in nuclear fuel. The fission fragment enters the lattice at left as shown by the arrow mark (Kopelman 1959).

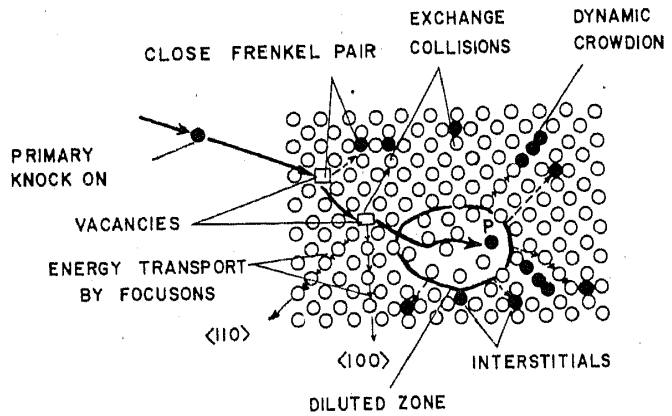

Figure 2. Schematic picture illustrating the formation of different types of lattice defects by a primary knock on atom. The knock-on atom enters the lattice at left and comes to rest at P (Chadderton and Torrens 1969).

and new transport processes are induced at quite low temperatures. The two basic types of lattice defects, namely, the vacancy and the interstitial recombine if the temperature is high. But they remain as single defects at lower temperature and have a large effect on the fuel element behaviour.

(iii) *Impurity atoms*: Each fission event creates two atoms of fission products which are chemically different from the original material. Presence and build-up of these impurity atoms influence properties of the fuels and a detailed study of the fission products is therefore very important.

3. Irradiation effects in metallic fuel

Uranium metal exists in three allotropic modifications with different crystallographic structure: Orthorhombic alpha uranium upto 668°C, tetragonal beta uranium (668–775°C) and body-centred cubic gamma uranium (775–1130°C). Most metallic uranium fuels are used in the alpha state. Orthorhombic alpha uranium shows highly anisotropic thermal expansion and exhibits poor dimensional stability during irradiation. The dimensional changes in alpha uranium result from three types of irradiation-induced phenomena: irradiation growth, irradiation creep and fission product swelling.

3.1 *Irradiation growth*

Irradiation growth refers to the change in uranium shape at constant volume without any external stress application. The phenomena of growth were reported by Konobeevsky *et al* (1955), Paine *et al* (1955) and Pugh (1955).

During irradiation a single crystal of alpha uranium exhibits growth in ⟨010⟩ direction, shrinkage in ⟨100⟩ direction and remains unchanged in ⟨001⟩ direction. In a polycrystalline sample the extent of dimensional changes depend upon the degree of preferred orientation in the specimen. The growth of uranium is expressed by the following correlation (Robertson 1969):

$$L = L_0 \exp(Gf),$$

where L is the length of specimen after a fraction f of the atoms have fissioned, L_0 is the initial length of the specimen and G is the growth constant. The value of G denotes the susceptibility of uranium to growth and depends upon uranium texture and irradiation temperature. Growth constant G has very large values at low temperature (sub-zero temperature) but relatively independent of temperature in the range 0–300°C and small values at high temperatures (Buckley 1964). No growth is observed at temperatures above 500°C.

The phenomena of irradiation growth is connected with the anisotropic thermal expansion of the alpha-uranium (figure 3). The direction of growth in uranium coincides with the direction which has a negative coefficient of thermal expansion. Similarly the direction which shrinks during irradiation corresponds to the direction of highest thermal expansion coefficient. The mechanism of irradiation growth involves formation of extra monolayer plates of lattice defects created by the passage of fission fragments in solid uranium on certain crystal planes (figure 4). The thermal stresses due to anisotropic expansion of uranium in the fission spike, force the vacancies and interstitials to aggregate on different crystal planes to cause elongation (due to interstitial clusters) in the direction ⟨010⟩ and contraction (due to vacancy cluster) in

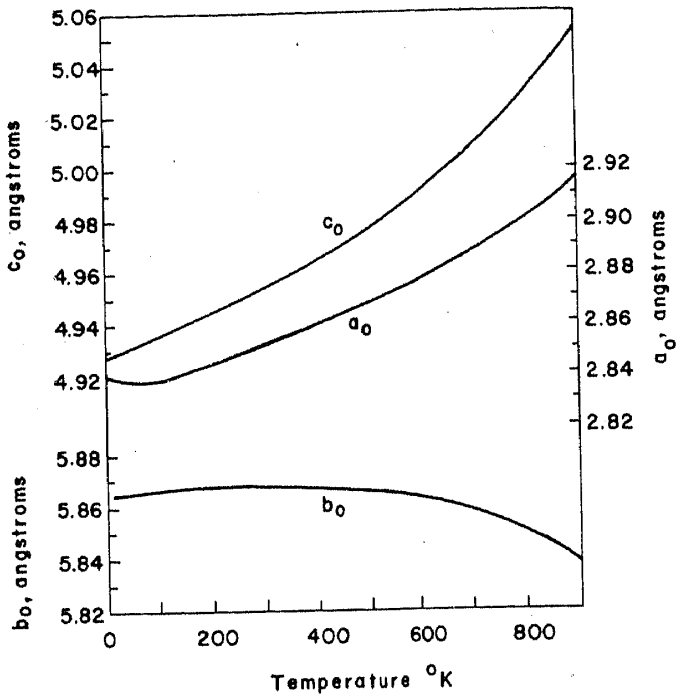

Figure 3. Lattice parameters of alpha uranium as a function of temperature (Holden 1958).

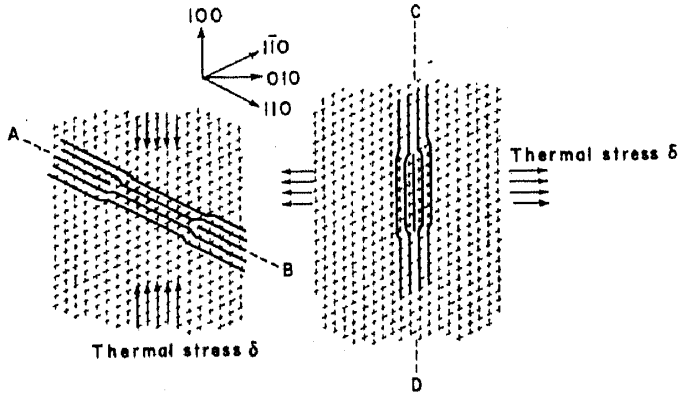

Figure 4. Projection of the alpha uranium lattice on (001) plane showing deformation caused by collapsed aggregate of vacancies on a (110) plane AB and a disc of interstitial atoms on a (010) plane CD, (Ostberg 1965).

⟨100⟩ direction. At higher temperature (above 500°C) the point defects created in uranium are sufficiently mobile to get annhilated and hence no growth is observed.

Since growth is enhanced by preferred orientation the only way to control growth is to have a random texture. This is obtained by beta-quenching of uranium which assures fine randomly oriented grains in the fuel.

3.2 *Irradiation creep*

Irradiation creep and irradiation growth play an important role in the often observed bowing of the uranium fuel element during irradiation (figure 5).

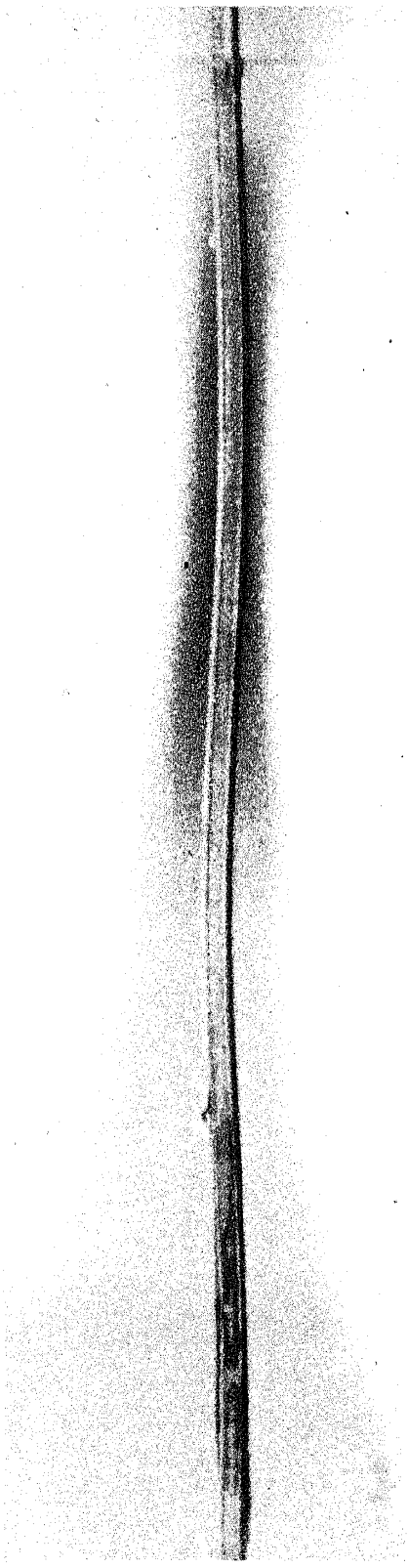

Figure 5. Bowing observed in an experimental uranium fuel element of *Dhruva* reactor (irradiated in CIRUS).

Accelerated creep of uranium during irradiation was reported by Konobeevsky *et al* (1955). It was found by Roberts and Cottrell (1956) that in a thermal neutron flux of 10^{12} n/cm^2/sec at temperature of 100°C, a stress as low as 1 % of yield strength caused appreciable creep in polycrystalline uranium. This observation was explained on the basis of yielding creep mechanism (figure 6). In this mechanism creep is caused by build-up of high internal stresses between the grains due to growth of misaligned grain in a polycrystalline material. When the internal stress reaches the yield stress, the material deforms plastically under the influence of an externally applied stress which is small compared to the yield stress. Most of the work is done by internal stress, the external stress merely guides the deformation. The creep rate due to this mechanism is given by the following correlation (Gilbert 1971)

$$\dot{\varepsilon}_c = (\sigma/\sigma_y)\dot{\varepsilon}_g,$$

where $\dot{\varepsilon}_c$ is irradiation creep rate, σ_y is the yield stress, $\dot{\varepsilon}_g$ is the growth strain rate and σ is the applied stress.

The dependence of creep rate on neutron flux and temperature is contained in the growth strain rate.

Another mechanism of irradiation creep in uranium deals with relaxation of elastic stress in the crystal lattice volume temporarily disorganised by a fission spike (figure 7). The creep rate due to this mechanism is given by the following correlation (Dienst 1977).

$$\dot{\varepsilon}_c = \frac{\sigma}{E}\dot{F},$$

where σ is the stress, E is Young's modulus and $\dot{F}$ is the fission rate.

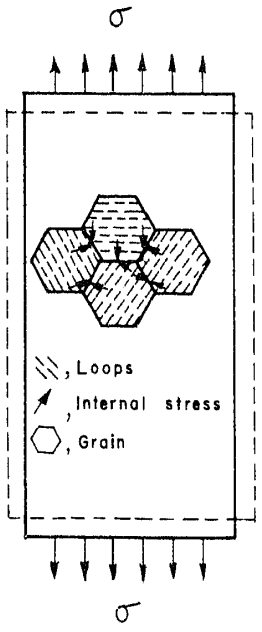

Figure 6. Yielding creep mechanism. Irradiation growth of misaligned adjacent grains produces internal stress (Gilbert 1971).

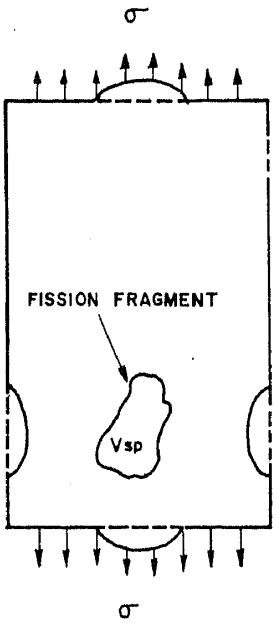

Figure 7. Relaxation of elastic stress in a fission spike. Arrows indicate stress, broken lines indicate initial specimen shape, solid lines indicate final specimen shape, v_{sp} is volume of spike (Dienst 1977).

3.3 *Swelling*

Swelling due to replacement of uranium atom by fission products was calculated by Howe and Weber (1957) who showed that the percentage volume increase in uranium should be about three times the atom percent burn-up. This estimate compares well with the swelling at lower temperatures where gaseous swelling is absent. However, large amount of swelling is observed in high purity uranium in the temperature range 350–600°C. A breakaway swelling (swelling maxima) is observed at about 450°C and the magnitude of swelling is more in high purity uranium compared to the swelling in uranium containing small amount of impurities (figure 8). Swelling in the temperature range 350–500°C is characterised by formation of large (50–200 microns) cavities and tearing at grain boundaries and at twins (Pugh 1955). In temperature range 500–600°C, swelling is associated with formation of small platelike pores crystallographically aligned in planar arrays within uranium grains (Legget *et al* 1964). The burn-up at which enhanced swelling appears in uranium depends on the temperature of irradiation. At higher temperature of irradiation, the swelling initiates at low burn-up but when the temperature is low the breakaway swelling can be delayed upto a high burn-up. External restraint is found to suppress the formation of cavities and aligned pores, reducing fuel swelling. Minor addition of alloying elements Fe, Al, C, Si etc in uranium inhibits the swelling.

Metal fuels operate at lower fractions of their melting points where fission gas diffusion is fairly slow. Moreover, the thermal gradient across the fuel is small due to higher thermal conductivity and the driving force for directed bubble migration is small. Bubbles generally remain quite small and gas release is negligible. The swelling of uranium originates from the nucleation and growth of bubbles of fission gases xenon and krypton which are insoluble in fuel matrix and tend to precipitate as bubbles on

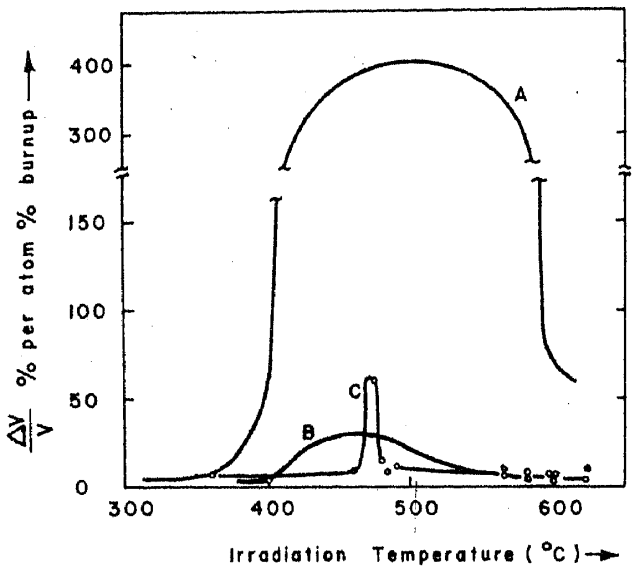

Figure 8. Swelling during irradiation as a function of temperature, A—high purity uranium. B—normal purity uranium. C—adjusted uranium (Robertson 1969).

grain boundaries, dislocation and twins. However, the anisotropic growth of uranium is considered to be the main driving force (in temperature range 350–500°C) for the formation of cavities and tears which are responsible for large swelling in uranium. The cavities are nucleated at the existing fission gas bubbles. Alternatively the cavities can be nucleated mechanically by the intergranular stresses arising from anisotropic growth of adjacent grains. When the gas bubbles or grain boundary tears exceed a critical size (2000 Å), they rapidly grow to form large cavities. The growth occurs by migration of vacancies to the cavity under the influence of tensile stress caused by intergranular interaction resulting from anisotropic growth of uranium. In the temperature range 500–600°C where irradiation growth is negligible, the swelling is believed to be caused by homogeneous nucleation of voids by condensation of vacancies (McDonell 1973). The suppression of swelling by addition of alloying elements is attributed to interaction of point defects with alloy constituents.

At one time it was thought that the swelling of metal fuels was sensitive to the fuel strength and therefore could be reduced by making stronger fuels with addition of alloy elements like molybdenum. It was, however, recognised later that the main restraining force on gas bubbles was surface tension rather than the matrix strength. Hence, keeping the gas bubbles smaller *e.g.* by providing numerous nuclei on which they can form rather than strengthening the matrix, could be more effective.

4. Irradiation effects in ceramic fuels

In addition to the intense radiation field, the ceramic fuels are exposed to very severe thermal conditions. Volumetric fission heat generation in ceramic fuels gives rise to large temperature difference between the centre line and external surface of the fuel elements. A typical mixed oxide fuel operates with a high centre temperature approaching melting point and there exists a radial thermal gradient as high as

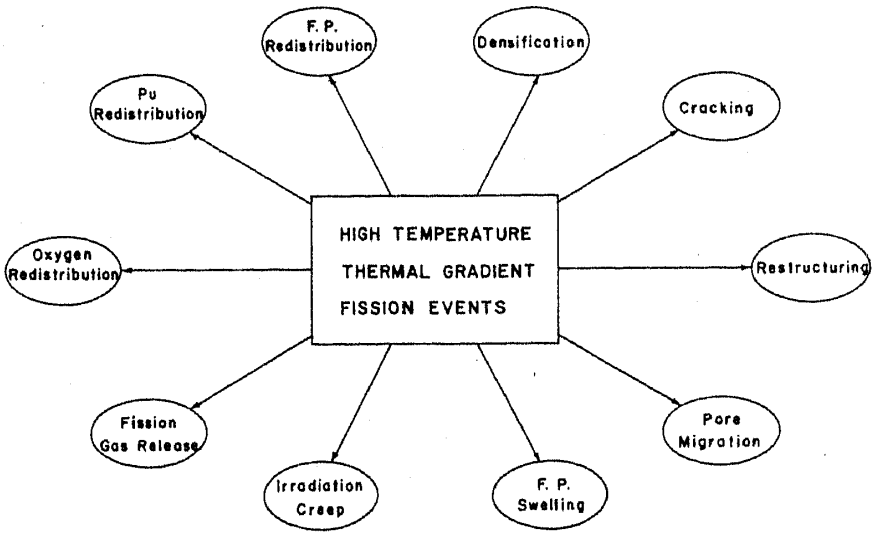

Figure 9. Changes observed in ceramic fuels during irradiation due to severe thermal and radiation environment in the fuel pellets (Roy and Sah 1983).

3000–5000°C/cm. Besides causing cracking and distortion of the fuel pellets as a result of thermal stress, these unique irradiation conditions provide the driving force for several transport processes in fuel which lead to significant changes in the microstructure, composition, dimension and shape of the fuel. The main irradiation effects (figure 9) can be divided in the following broad categories: (a) densification; (b) restructuring; (c) redistribution of fuel and fission products; (d) effects of fission gases: swelling and gas release; (e) irradiation creep

4.1 *Irradiation-induced densification*

The problem of irradiation-induced densification which results in formation of large axial gaps in the fuel column and leads to collapse of cladding tube in these gaps, was first observed in 1972 in large pressurised water reactors (PWRS). This sent a shudder through the reactor engineers who had to derate the reactor power pending investigations into the mechanism and possible solution of fuel densification under irradiation. Fortunately, within a short period the mechanism was correctly identified which defined the requisite microstructure (consisting of large grains and controlled porosity) of a densification resistant fuel. Use of densification resistant fuel along with internal prepressurisation of the fuel element provided a satisfactory solution to the problem.

The densification of ceramic fuels during irradiation is caused by fission spike-pore interaction which results in shrinkage and dissolution of pores present in the fuel matrix (figure 10). It takes place quite early in life and has much greater technological significance. Irradiation-induced pore shrinkage and annihilation was observed by Wapham (1966) using electron microscope. Later Ross (1969), Bellamy and Rich (1969) and Turnbull and Cornell (1970) reported similar observations. A fission fragment traversing through fuel grain disrupts the pores on its track. The pore is transformed into lattice vacancies in this process. The vacancies generated in this event migrate to the nearby pores, or to the grain boundaries. Vacancy migration to the grain boundary results in densification of the fuel. Due to large number of vacancies generated by one

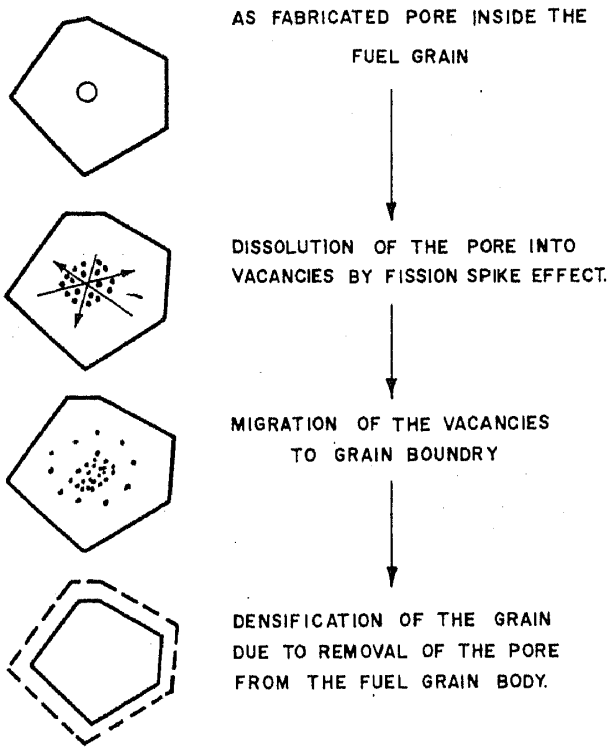

Figure 10. Mechanism of in-pile fuel densification (Chubb *et al* 1975).

fission event and large fission rate (10^{13} fissions/c.c), the rate of densification is considerable.

Assman and Stehle (1978) derived an equation for volume change in fuel due to densification. They considered two populations of pores in the fuel body, coarse pores which are relatively stable and fine pores ($< 0{\cdot}1$ μm) which are atomised in a single encounter with fission spike. Assuming densification to occur by flux of vacancies from grain body to the grain boundaries they gave a correlation of the following form for the volume change ($\Delta V/V_0$) in the fuel:

$$\Delta V/V_0 = -f^* P_0 [1 - \exp(-n^* \Omega_s F_t)],$$

where

$$f^* = \frac{1}{1 + (4\pi/15) Z_c r_c r_g^2},$$

and

$$n^* = (1 - (4\pi/45) Z_p r_p r_g^2) n.$$

In the above correlation Ω_s is volume of fission spike, F_t is burn-up in fission/c.c, n^* is the fraction of vacancies per encounter that can escape from the fine pores. The factor f^* ($\leqslant 1$) describes the effect of coarse pores which capture a fraction of vacancies produced. r_c is radius of coarse pores, r_g is grain size (radius), Z_c and Z_p are densities of coarse and fine pores respectively, P_0 is initial porosity. For very small initial concentration of fine pores in the fuel body $f^* = 1$ and $n^* = n$. The above correlation shows an exponential law for pore removal from fuel and it also brings out the important parameters which have significant effect on in-pile fuel densification.

4.2 *Fuel restructuring*

The microstructure of the unirradiated sintered ceramic fuel pellet consists of the equiaxed grains of 5–15 micron diameter with uniformly distributed porosity. The cross-section of irradiated fuel however, reveals concentric zones of altered microstructures (figures 11 and 12) which are indicative of the temperature in the fuel during irradiation. These zones have fairly-defined temperatures associated with their boundaries. The different microstructural zones and the temperature range in which they are formed in mixed oxide and mixed carbide fuels are listed in table 1. Equiaxed grain growth law is given by the following correlation (Olander 1976):

$$D^m = D_0^m + K_0 t \exp(-Q/RT)$$

where D and D_0 are the final and the initial grain size, K_0 is a constant, t is time, Q is activation energy and T is temperature. The exponent m and the activation energy were found to be 2·5 and 460 kJ/mol respectively for UO_2 in laboratory experiments. Under irradiation conditions, the presence of fission gas bubbles on grain boundary has a retarding effect on grain growth rate. Ainscough *et al* (1973) suggested the following grain growth law for UO_2 during irradiation:

$$\mathrm{d}(D)/\mathrm{d}t = k\left(\frac{1}{D_0} - \frac{1 + 2000\Omega\dot{F}t}{D_m}\right)$$

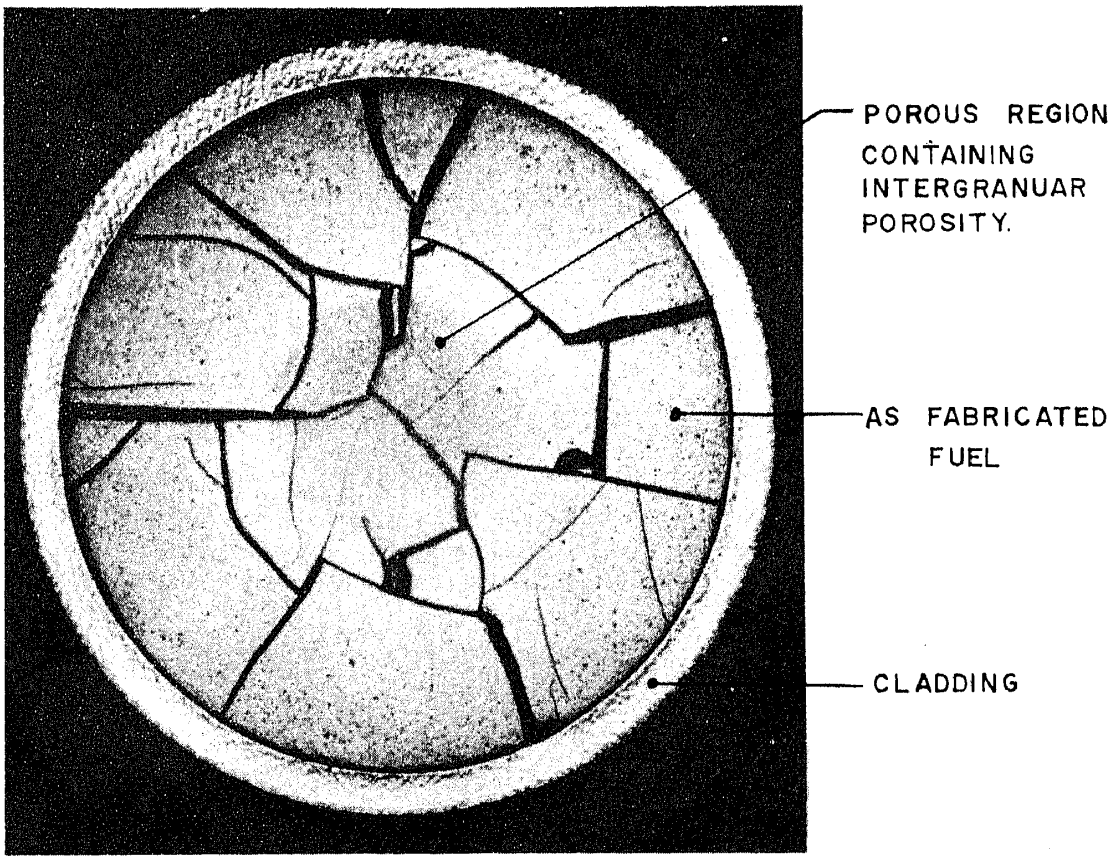

Figure 11. The cross-section of the irradiated UO_2 fuel element of Tarapur Atomic Power Station (TAPS) revealing formation of a porous central region in the fuel pellet, (magnification 6X). The maximum fuel centre temperature was estimated to be 1250°C (Bahl *et al* 1979).

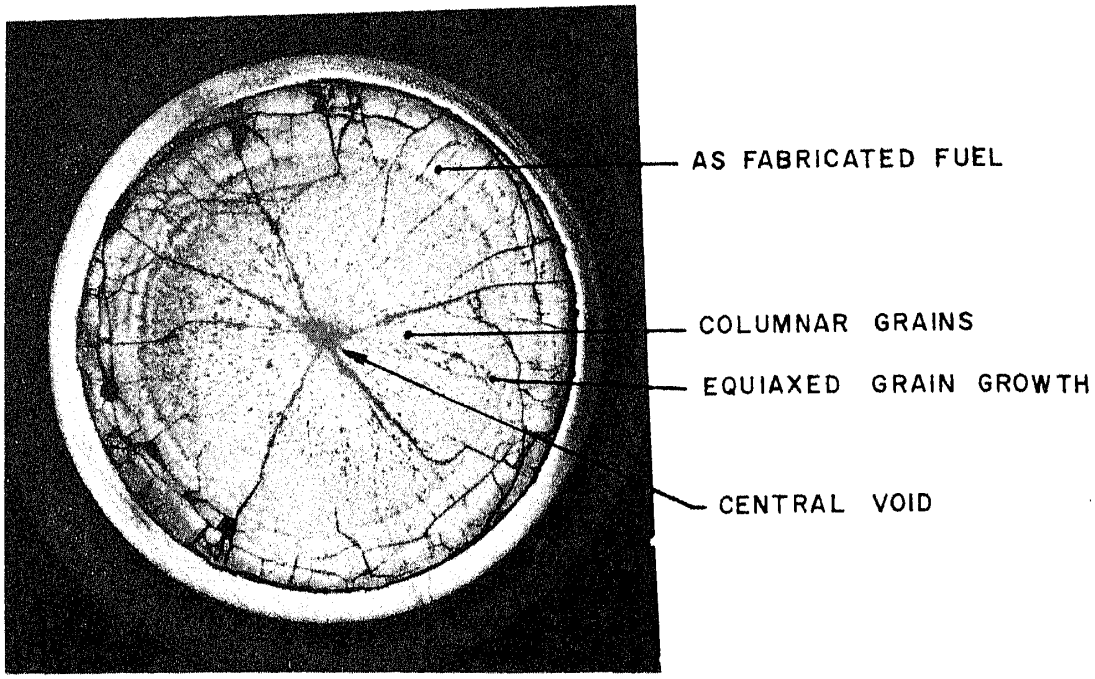

Figure 12. Restructuring observed in fuel pellet of Tarapur Atomic Power Station (magnification 5X). The maximum fuel centre temperature was estimated to be 2200°C.

Table 1. Microstructural zones observed in the cross-section of an irradiated ceramic nuclear fuel pellet.

Fuel type	Temperature range	Microstructural observations
$(U, Pu)O_2$	below 1100°C	As sintered microstructure
	1100–1300°C	Intergranular porosity
	1300–1700°C	Equiaxed grain growth
	Above 1700°C	Columnar grain growth and central void
(U, Pu)C	below 1100°C	As fabricated microstructure and very small bubbles
	1100–1400°C	Grain growth, large gas bubbles, bubbles at grain boundaries
	1400–1700°C	Radially elongated grains and pores
	Above 1700°C	Irregular, big rounded pores and central void

where D_m is limiting grain size, k is the grain growth constant, $\dot{F}$ is fission density and Ω is atomic volume. Formation of radially oriented columnar grains involves movements of pores up the temperature gradient by an evaporation and condensation mechanism. Fuel on the hotter side of a large lenticular pore evaporates and condenses on the cooler side creating a transport process for the pores to migrate up the thermal gradient. The movement of the pores to the centre of the fuel results in high density columnar grains and the formation of a central hole or 'void'. It can take as little as 24 hours at power for

restructuring to occur. The rate of columnar grain growth is governed by temperature and thermal gradient. The process is important at temperatures where the vapour pressure of the ceramic fuel becomes significant.

4.3 *Redistribution of fuel constituents and fission products*

4.3*a Plutonium redistribution*: Plutonium-bearing ceramic fuels initially contain uniformly distributed plutonium. During irradiation, however, plutonium tends to segregate to some preferred locations. In mixed oxide $(U, Pu)O_2$ fuel the segregation of plutonium is observed to be related to the initial stoichiometry of the fuel. The radial profile of plutonium concentration measured in an irradiated mixed fuel of two different initial stoichiometry, showed that in fuel having an initial O/M of 2·01 the plutonium segregated towards fuel centre while in fuel having an initial O/M of 1·935 the plutonium segregation occurred away from the fuel centre (figure 13). This indicated the possibility of the existence of a critical value of stoichiometry for which no plutonium segregation should occur. However, plutonium will segregate towards periphery or towards centre depending upon the fact whether the initial O/M of fuel was lower or higher than the critical value respectively.

The observed plutonium segregation is successfully explained by vapour transport mechanism which involves preferential evaporation and migration of one of the fuel species. The basis for vapour transport mechanism is migration of lenticular pores towards fuel centre by evaporation and condensation of fuel material. The plutonium segregation is caused by the difference in the U/Pu ratio in the solid and its vapour inside the migrating pore. When the O/M ratio of the fuel is such that congruent evaporation can take place then no plutonium segregation will occur. If the stoichiometry is higher (than the stoichiometry for congruent evaporation) the vapour

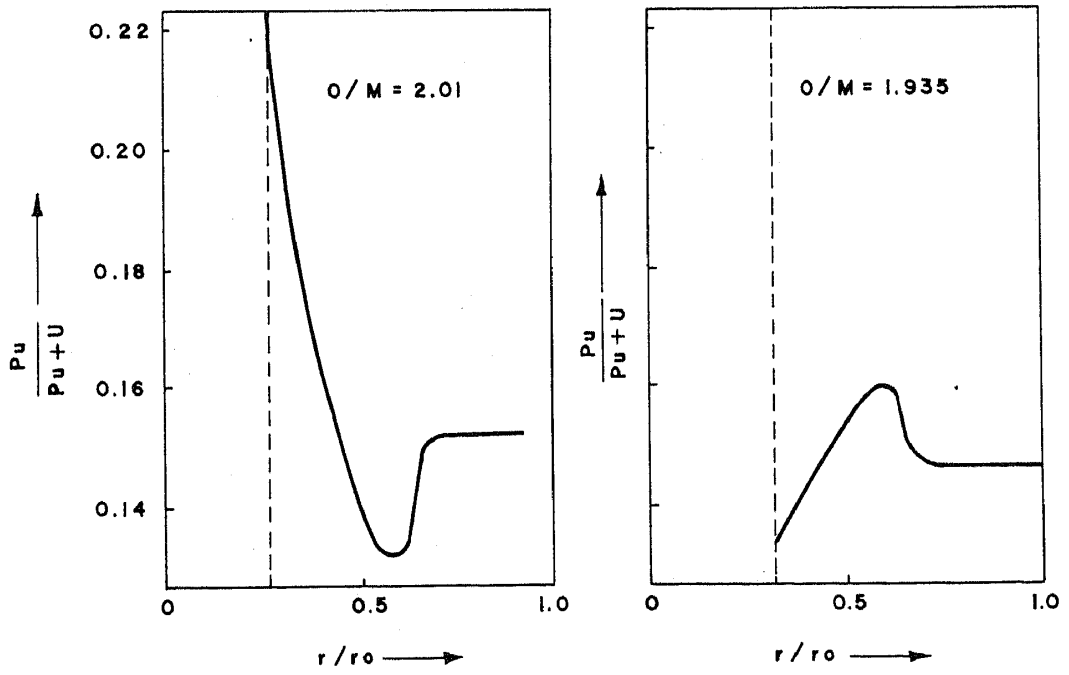

Figure 13. Radial plutonium profile observed after irradiation in mixed oxide fuels of two different O/M ratios (Bramman and Powell 1975).

phase in the pore consists almost entirely of UO_3 with minor amount of UO_2 and PuO_2. This leads to preferential migration of uranium from high temperature central region making the centre rich in plutonium. When the O/M of the fuel is lower, the vapour phase inside the pore consists of PuO which leads to depletion of plutonium from the centre. Attempts have also been made to explain the redistribution of plutonium on the basis of solid state thermal diffusion of plutonium (Beiswenger *et al* 1967; Bober *et al* 1969). Though it was possible to predict plutonium segregation towards centre, the mechanism of thermal diffusion cannot explain the reversal in the direction of plutonium segregation observed at low O/M ratio.

4.3*b* *Oxygen redistribution*: In a mixed oxide fuel containing appreciable amount of plutonium, oxygen also gets redistributed under the influence of radial thermal gradient. The oxygen migration in the fuel is governed by the initial stoichiometry of the fuel. In a hypostoichiometric fuel, the oxygen migrates towards the low temperature side (*i.e.* towards fuel periphery) while in a hyperstoichiometric fuel the oxygen migration occurs from low temperature to high temperature side (figure 14). In both cases, the fuel surface tends to approach stoichiometry.

The redistribution of oxygen observed in the mixed oxide fuel is explained by two mechanisms (Olander 1976): (i) oxygen transport in gas phase by counter diffusion of CO_2 and CO, (ii) thermal diffusion of oxygen vacancies. The mechanism of oxygen transport through gas phase is based on the attainment of a thermodynamic equilibrium among CO_2, CO and oxygen in the existing temperature gradient. The gases CO and CO_2 are formed from the carbon impurity in the fuel. In a hyperstoichiometric fuel the CO_2 diffusing to the hotter zone releases an oxygen atom to the solid and the CO formed diffuses back to the cooler zone where it picks up an

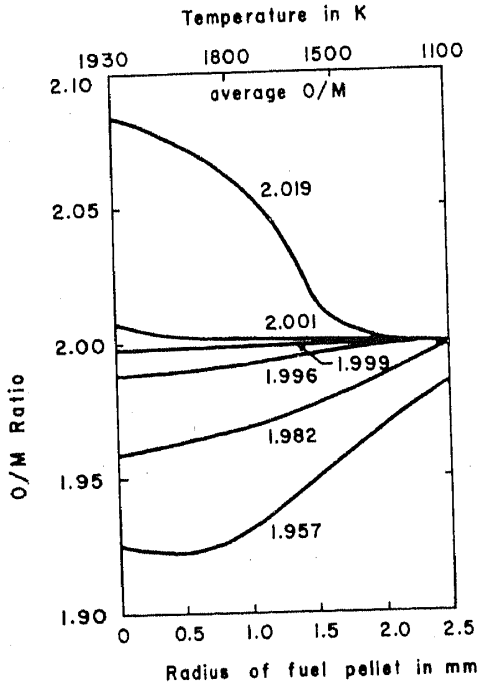

Figure 14. Redistribution of oxygen in mixed oxide fuel pellet of different initial stoichiometry (Assman and Stehle 1982).

oxygen atom to form CO_2 which repeats the cycle. This happens till a constant CO_2/CO ratio determined by the initial composition of the fuel is achieved.

The above model meets with difficulty when applied to transport in the hypostoichiometric fuel. The very low oxygen potential of hypostoichiometric fuel does not allow complete gasification of available carbon. So CO_2 pressure is very low. Therefore the CO/CO_2 mechanisms would be extremely slow in hypostoichiometric fuels. However, experiments have shown a rapid oxygen redistribution in hypostoichiometric fuels. This indicates that other mechanisms may be responsible. Therefore, a model of oxygen transport by thermal diffusion of oxygen has been proposed. In this model the diffusing species are considered to be single oxygen vacancies. The heat of transport for these species being negative, they migrate towards high temperature region.

4.3*c Fission product redistribution*: The fission process in nuclear fuel results in production of atoms of more than 30 elements and about 120 isotopes of these elements have appreciable half lives. Due to steep temperature gradient in the fuel some fission products move away from the location where they are produced. Loss or gain of fission products from the region where they were created, alters many important physical and chemical properties of the fuel locally. The effect of fission products on the fuel behaviour is governed by their physical and chemical state. One of the important consequence of fission product redistribution is the possibility of chemical attack by fuel on the cladding material.

Studies of fission product distribution in irradiated oxide and mixed oxide fuel have provided the following important findings: (i) Fission product elements Zr, Nb, Ce, Pr, Ba and Sr which exists as non-volatile oxide in solid solution with the fuel, do not redistribute. (ii) Noble metals Ru, Rh, Pd and a part of Mo exist in elemental form and migrate significantly. They are observed as white metallic inclusions in the columnar grain zone or as alloy in the central void. (iii) Volatile fission products Cs, Rb, I, Te, Sb and Cd tend to migrate to the cooler regions in the fuel. Gross radial migration of cesium occurs from high temperature central regions to cooler periphery fuel and to the pellet interface locations. Axial migration of cesium to the plenum is also observed. This migration behaviour of cesium is attributed to its high volatility. (iv) In fuels containing appreciable amount of plutonium, the fission yield of noble metals is higher and the yield of oxide forming elements is lower compared to their yield in uranium fuel. Due to this effect, a part of oxygen released by fission, remains in uncombined form in the fuel and increases its oxygen potential.

4.4 *Effects of fission gases*

A substantial fraction (15%) of the fission products in nuclear fuel consists of rare gases, xenon and krypton, which have extremely low solubility in the fuel matrix. If these gases are released from the fuel body they increase the pressure inside the fuel element subjecting the cladding tubes to stress. On the other hand, if they are retained in the fuel, they precipitate as gas bubbles and cause fuel swelling. The dimensional changes in fuel due to swelling leads to mechanical interaction between the fuel and cladding which often leads to pellet clad interaction failure by stress corrosion cracking (figure 15).

4.4*a Fission gas swelling*: Swelling of the fuel is attributed to the volume of fuel occupied by the gas bubbles. Bubble formation depends on the mobility of gas (either as

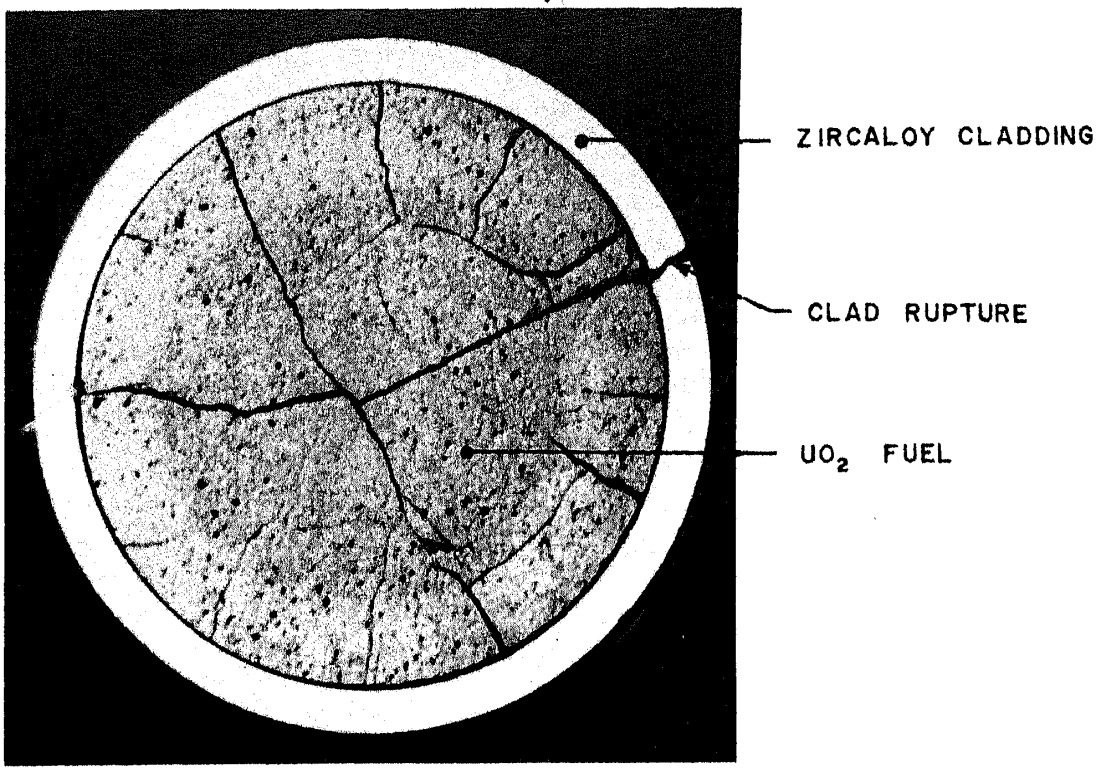

Figure 15. Cross-section of a failed UO_2 fuel element from TAPS which was examined at BARC. The rupture of the cladding was caused by stress corrosion cracking (Bahl *et al* 1979).

single atom or complexes), the minimum number of gas atoms required to form a stable nucleus and the rate at which lattice vacancies can be supplied to enhance the stability of a nucleated complex. In the irradiation environment existing in the fuel the nucleation and growth of gas bubbles is accompanied by the irradiation induced re-solution of bubbles by fission fragments. It is known that bubbles which are stable out-of-pile are susceptible to re-solution in irradiation environment even at temperature as high as 1200°C.

The nucleation of bubbles occurs heterogeneously on the fission fragment tracks (Turnbull 1971). The nucleation sites are believed to be vacancy-rich segment of the fission fragment tracks. Such nucleation is independent of thermally activated transport properties and is therefore intrinsically unaffected by temperature, which is in agreement with the observations of Cornell (1971) who showed that density of intragranular bubbles is insensitive to temperature. Since two xenon atoms form a thermally stable nucleus, homogeneous nucleation of gas bubbles has also been considered but in this case bubble density will depend on temperature which is opposed to the observations of Cornell.

Bubbles nucleated under irradiation grow by capture of gas atoms and vacancies and then get dissolved by irradiation induced re-solution (Turnbull 1971). Concentration of intragranular bubbles is sustained by fresh nucleation. There is a dynamic equilibrium between formation of gas bubbles by nucleation and growth on one hand and resolution of the bubbles by fission fragments on the other. At temperatures above 1200°C the resolution becomes less effective because of the increased gas atom mobility. The growth of bubbles depends on the temperature (which determines the gas diffusion

coefficient) and burn-up which controls the dissolved gas atom concentration. Because of the re-solution process each bubble has an average life defined by

$$T \simeq [1/2\pi r^2 F \lambda],$$

where r is bubble radius, F is fission rate and λ is range of fission fragment. This indicates that the bubble growth is restricted. However, the observed presence of large gas bubbles in the fuel suggested that bubbles larger in size are more stable because the re-solution is not so effective in destroying large bubbles as it is with small bubbles. Turnbull and Cornell (1970) showed that bubbles with diameter greater than 24 Å have enhanced stability as they cannot be destroyed in a single event of bubble-fission fragment interaction.

The equilibrium number of bubble per unit volume, n in the fuel is given by

$$n/T = 2F\alpha,$$

where α is number of bubbles nucleated per fission fragment, T and F have the same meaning as in earlier equation.

The equilibrium quantity of gas m in intragranular bubbles per unit volume of fuel is given by following correlation (Turnbull 1971):

$$m = (4\alpha/3\lambda b')\,(2b'CD/\pi F\lambda)^{1/4},$$

where b' is Van der Waals constant for fission gas, C is dissolved gas atom concentration, D is gas diffusion coefficient, F, λ and α have same meaning as earlier. This indicates that the quantity of gas in intragranular bubbles increase as fourth root of the dissolved gas concentration. It is clear that the fraction of gas in the intragranular bubble is invariably a small fraction of the entire gas content. The importance of this fact is that the gas from the matrix migrate to grain boundary as single atom and forms intergranular bubbles. In fact a major part of the swelling observed in fuel is caused by formation and growth of large intergranular bubbles in the process of gas release.

Metallographic observations (Chubb 1972) on UO_2 irradiated at temperature below 1600°C showed an equiaxed grain structure with extensive porosity along the boundaries where fuel temperatures was sufficiently high. This porosity accounts for the majority of the fuel swelling. Detailed investigations of intergranular fractured surfaces show the characteristics of bubbles lying on grain faces and those situated at grain edges and corners. The latter are observed to be extensively developed and generally occupy a larger volume than the relatively small grain face bubbles.

4.4*b* *Fission gas release*: Release of fission gases from the fuel to the free volume of the fuel elements is governed by the mobility of the gas as individual atoms or as bubbles in the existing condition during irradiation. The release of fission gases is observed to be strongly dependent on temperature. Other factors which influence the release are grain size, burn-up, fission rate, fraction of open porosity, fuel density and stoichiometry of fuel in UO_2.

Xenon is found to diffuse in UO_2 as a complex of constant size. This complex consists of a xenon atom bound with one uranium vacancy and two oxygen vacancies. The diffusion of xenon has been studied by Cornell (1969). It is found that xenon has no significant mobility in UO_2 at temperatures below 1000°C. Migration of bubbles may occur by several processes. The effective diffusion coefficient for migration of gas bubble at a constant temperature is dependent on its radius (r) and is proportional to

r^{-n} (Gittus 1978) where the exponent is dependent on the physical process responsible for bubble movement. The value of n is 4 for surface diffusion, 3 for volume diffusion and 2 when bubble movement occurs by diffusion of atoms in a vapour phase across bubble filled with equilibrium pressure of insoluble gas. It is found that under the effect of temperature gradient surface diffusion is the dominant mechanism of migration for bubbles with radii less than 16 microns. Bubbles of larger (> 16 micron) size move by vapour transport mechanism. However, no bubble migration is observed at temperatures below 1500°C and the main mode of gas mobility upto 1500°C remains atomic diffusion. The method of predicting gas release in terms of the diffusion coefficient alone is, however, not reliable because of the existence of different types of traps like dislocations, grain boundaries, bubbles, lattice defects, defects clusters, precipitates of fission products. Moreover, sudden changes in gas release with changes in reactor power have been observed which could not be accounted for by the diffusion processes. 'Gas burst' is observed to occur at start-up and shutdown and during power transients.

Two basic mechanisms of gas release operate below 1000°C. They are based on two collision processes, (a) 'recoil' in which a fission event near the surface produces a gas atom which has sufficient energy to escape from the solid, (b) 'knock-out' where a fission fragment collides with a gas atom with sufficient energy to knock it out of the solid.

In the temperature range 1000–1600°C the release occurs by atomic diffusion of gas atoms from grain interior to the grain boundaries (figure 16) where the ready supply of vacancies permits the gas atoms to form gas bubbles large enough to survive the re-solution effect. Bubbles on the grain boundary grow by collection of atoms from grain interior. If the temperature is sufficiently high to cause grain growth, the grain boundary sweeping of the fission gas atoms from the fuel provides additional gas at the boundary. The grain boundary bubbles grow at a rate determined by the supply of gas atoms at the boundary. A point is reached when the bubbles are large enough to interlink with each other representing grain boundary saturation with fission gases forming a continuous channel for release of the gas to open surfaces. Since the grain boundary saturation is a prerequisite for release of gases in this mechanism, there has to be an incubation period (threshold burn-up) before the gas release occurs. Threshold burn-up for gas release is a function of temperature; higher the temperature lower the burn-up when release starts. Several models of fission gas release (Collins *et al* 1973; Notley and Hastings 1980) have been developed using the above mechanism.

At temperature above 1600°C almost all the fission gas generated in the fuel is released. The release occurs by movement of gas bubbles which are sufficiently mobile at such high temperatures. The closed pores in the fuel also move up the gradient and sweep the fission gases on their way to the fuel centre where they are released to the central void. The above mechanism of pore and bubble migration for gas release is also responsible for formation of radially oriented columnar grains in the fuel.

In spite of large amount of theoretical and experimental work on fission gas release behaviour in ceramic fuels, the understanding of the mechanism is not complete. There is often a wide gap between the predictions and experimental observations of fission gas release especially in transient tested fuel elements (Pickman 1984). Intensive research in this field, however, unveiled some interesting phenomena in mid-sixties. A scientifically important discovery was that fission events could cause fission gas bubbles to redissolve into the lattice.

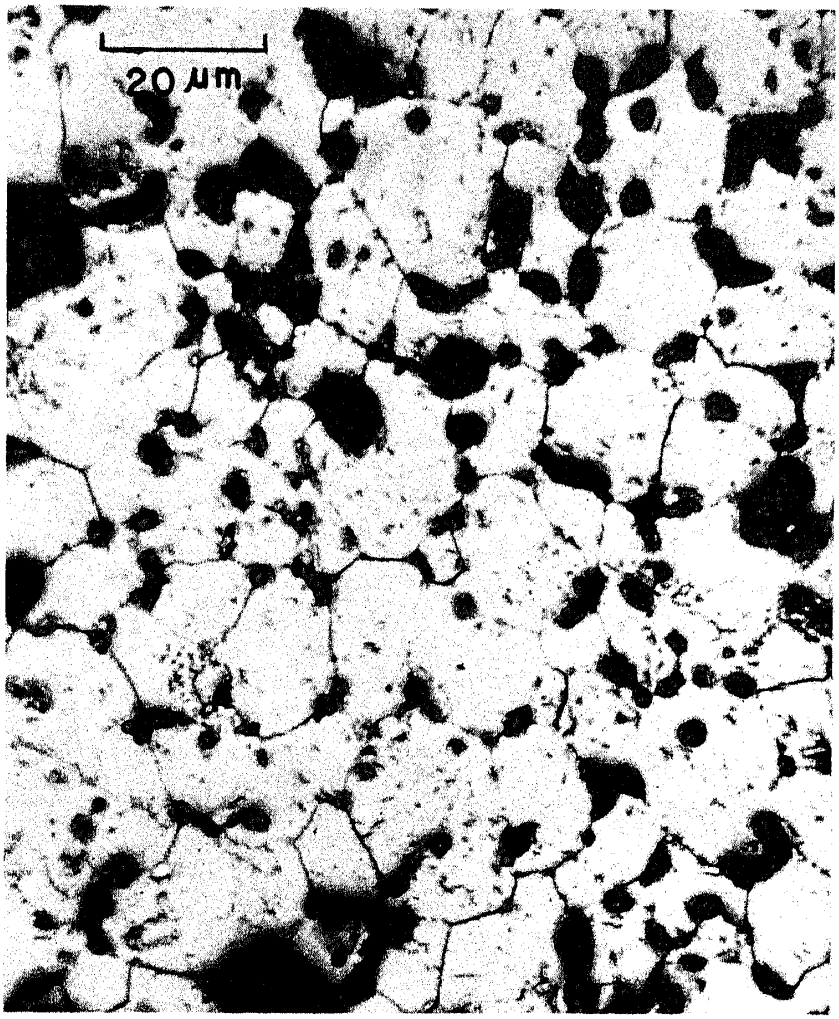

Figure 16. The microstructure of an irradiated UO_2 fuel from TAPS showing presence of fission gas bubbles on the grain boundary.

4.5 *Irradiation creep*

Irradiation creep plays a very important role in controlling the strain rate of cladding when fuel-cladding mechanical interaction starts in fuel elements at high burn-up. The effect of irradiation on creep of ceramic fuels is two-fold (a) to enhance the thermal creep, and (b) to develop creep under condition in which thermal creep is absent. UO_2 exhibits creep even at temperatures below 1100°C during irradiation (figure 17). The irradiation induced creep rate is observed to be a linear function of stress and fission rate. Several mechanisms have been proposed for irradiation creep in ceramic fuels (Dienst 1977; Gilbert 1971). The mechanisms proposed for irradiation creep fall in three categories (i) mechanisms based on diffusional creep (ii) mechanisms based on fission spike effect in fuel (iii) mechanisms based on growth of dislocation loops.

It was earlier thought that increase in vacancy concentration resulting from irradiation may enhance the volume self-diffusion term in Nabarro-Herring creep model and this was responsible for the enhancement of creep rate in the fuel. However it was shown (Olander 1976) that creep rate in Nabarro-Herring creep model does not get enhanced because the defects produced by radiation in the grain are either annihilated

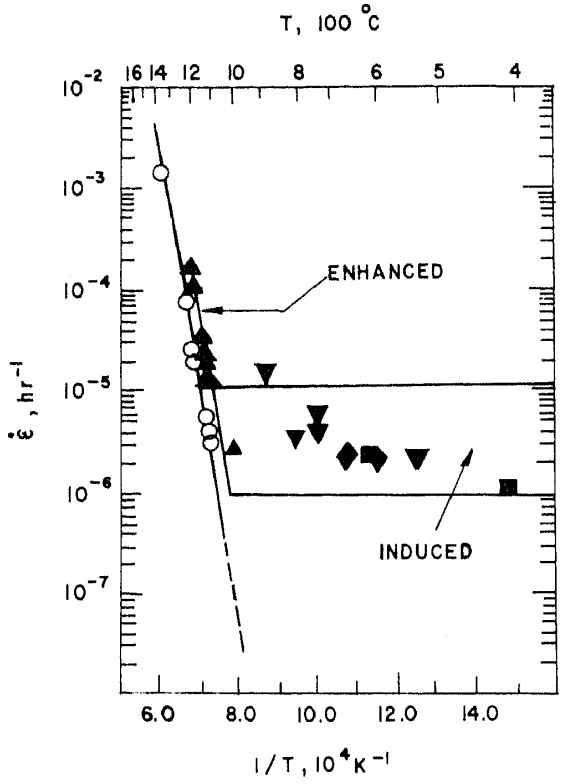

Figure 17. Irradiation creep rate of UO_2 as a function of temperature (Solomon *et al* 1971).

or flow equally to the grain boundary. Brucklacher considered that the point defects formed during irradiation anneal at the defects clusters present inside the grains. He replaced the grain of Nabarro-Herring model by defect clusters of 1000 Å size and was able to predict irradiation creep which was in agreement with the experiment. Another modified diffusional model presented by Brucklacher *et al* (1970) for irradiation creep considered diffusion of vacancies between dislocation loops formed during irradiation having different orientations relative to the stress direction. Tensile stress causes growth of loops which are normal to the stress, at the expense of loops parallel to the stress direction.

One of the spike-based mechanisms proposed that creep is accelerated by transient pulse heating of fuel by fission spikes. As the material in cylindrical region around the axis of the fission fragment track is momentarily brought to liquid state there is a very large increase in the vacancy diffusion coefficient which gives acceleration of creep. Perrin has proposed another mechanism based on spike effect which is applicable to irradiation enhanced creep in fuel. In this mechanism the fuel undergoes continuous annealing due to fission spikes; strain hardening is prevented and fuel creeps continuously in primary stage (figure 18). The creep rate is given by the primary thermal creep rate and is governed by temperature and fission rate. Creep is considered enhanced with respect to the secondary thermal creep rate which is normally lower than primary creep rate due to strain hardening. Besides the above mechanism the elastic stress relaxation mechanism described in §3.2 has also been proposed for ceramic fuels.

Dislocation-based creep mechanisms consider the formation and growth of dislocation loops under irradiation. It is considered that under the influence of stress

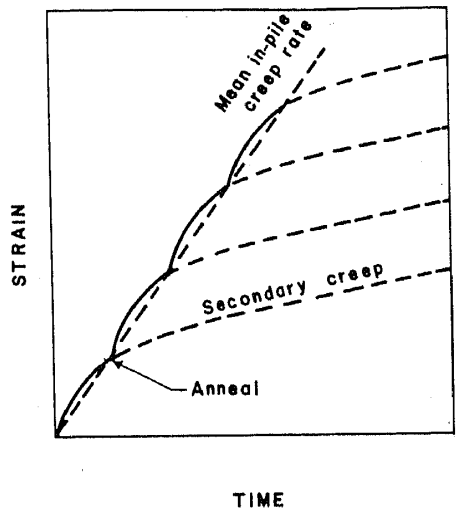

Figure 18. Maintenance of primary creep mechanism by fission spike annealing (Dienst 1977).

the irradiation-produced defect clusters collapse into dislocation loops preferentially on certain planes. Appropriately oriented loops grow by capture of interstitials. The creep rate in this mechanism is given as a function of stress and fission rate.

5. Prediction of fuel element behaviour

The behaviour of nuclear fuel elements during irradiation is a function of large number of processes which take place simultaneously and interact with each other in a complex manner. Figure 19 shows the complicated interrelation between various physical, chemical, mechanical and metallurgical phenomena which occur inside a water reactor fuel element. To predict the irradiation behaviour of the fuel element a computer model is needed which represents the interactive processes shown in this figure and allows a quantitative estimation of the evolution of changes in the fuel element. The computer model incorporates all the contemporary data of the material properties and the latest understanding of the phenomena and their mutual interactions. It is a very useful tool for design of fuel elements, safety analysis and for the interpretation of the results of irradiation experiments.

The analysis performed by fuel element computer models can be grouped in two categories: thermal analysis and mechanical analysis. The thermal analysis concerns the calculations of the fuel temperature distribution in the fuel set up by the volumetric heat generation. In a cylindrical fuel element, the steady state radial temperature distribution is obtained by solution of following equation with appropriate boundary conditions.

$$\frac{1}{r}\frac{\mathrm{d}}{\mathrm{d}r}\left(rk\frac{\mathrm{d}T}{\mathrm{d}r}\right)+H=0,$$

where k is the thermal conductivity of fuel which is a function of temperature and depends on fuel density. H is volumetric heat generation rate. The heat generation rate in thermal reactor fuel elements is not uniform along the fuel radius owing to thermal

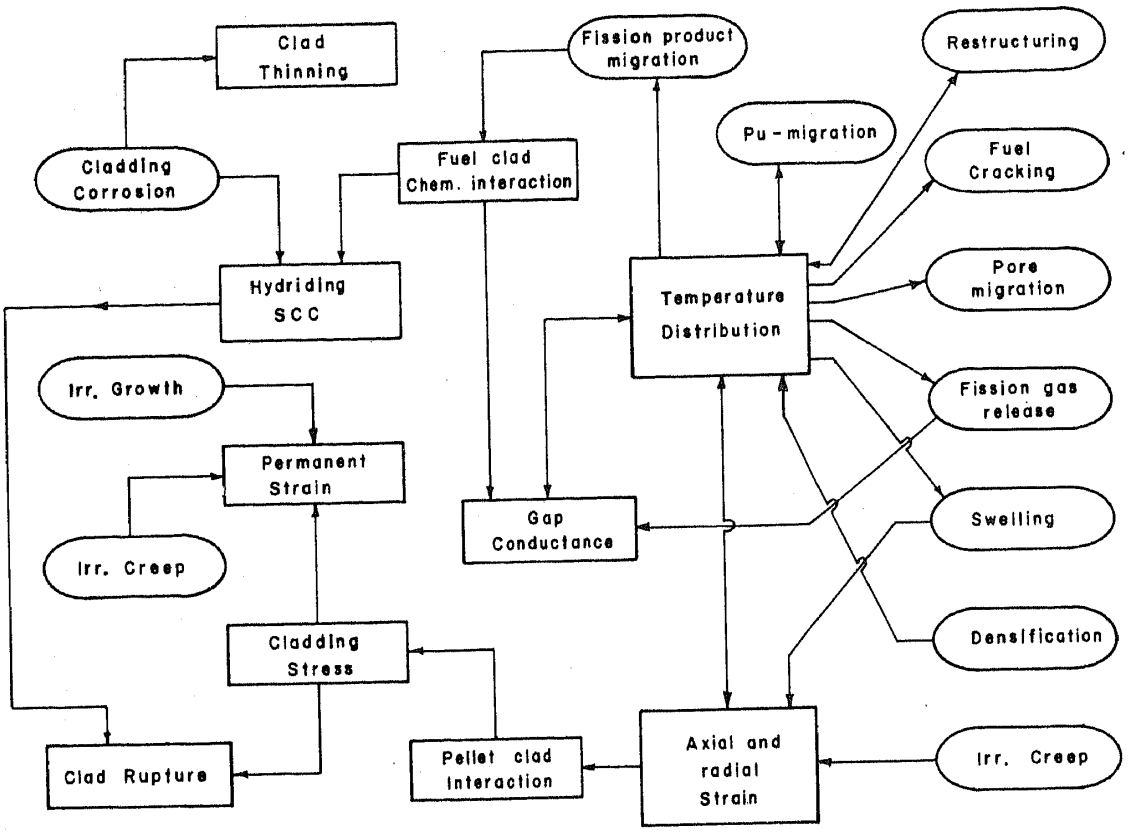

Figure 19. Interrelation of physical, chemical and metallurgical processes operating in a ceramic fuel element during irradiation (Sah *et al* 1983).

neutron flux depression towards the fuel centre. With the progress of irradiation, the magnitude and radial variation of fuel thermal conductivity (k) and heat generation rate (H) changes with time due to several irradiation effects *e.g.* porosity redistribution, fissile material segregation, restructuring etc. The temperature distribution is evaluated at small time intervals accounting for the irradiation effects in the fuel element.

One important aspect of calculation of temperature distribution in fuel is the heat transfer across the fuel cladding gap or interface. The fuel centre temperature is very sensitive to the gap conductance which governs the temperature drop in the fuel-clad gap. The heat transfer coefficient (h) for conduction of heat through the gas filled gap is given by

$$h = \frac{K_{\text{gas}}}{X_{\text{gap}} + g_i + g_f + \delta},$$

where K_{gas} is the thermal conductivity of the gas, X_{gap} is the fuel clad gap in operating conditions, δ is the sum of surface roughness of the fuel and the cladding, g_f and g_i are jump distance of the gas in fuel and cladding. The value of K_{gas} decreases considerably by the release of fission gas to the fuel clad gap since xenon has a very low thermal conductivity compared to helium which is used as a filler gas in the fuel element. The value of X_{gap} during irradiation is controlled by the processes responsible for gap closure *e.g.* densification, swelling and creep. Uncertainty in the prediction of gas release and fuel clad gap leads to uncertainty in the fuel temperature.

The mechanical analysis is carried out assuming axisymmetry and plane strain conditions. The total strain in the fuel and the cladding is considered to be composed of elastic, thermal, swelling, creep and plastic strains. The constitutive equations used in the modelling are

$$\varepsilon_r = \frac{1}{E}[\sigma_r - \nu(\sigma_\theta + \sigma_z)] + \varepsilon_r^{\text{th}} + \varepsilon_r^s + \varepsilon_r^c + \varepsilon_r^{\text{pl}},$$

$$\varepsilon_\theta = \frac{1}{E}[\sigma_\theta - \nu(\sigma_r + \sigma_z)] + \varepsilon_\theta^{\text{th}} + \varepsilon_\theta^s + \varepsilon_\theta^c + \varepsilon_\theta^{\text{pl}},$$

$$\varepsilon_z = \frac{1}{E}[\sigma_z - \nu(\sigma_r + \sigma_\theta)] + \varepsilon_z^{\text{th}} + \varepsilon_z^s + \varepsilon_z^c + \varepsilon_z^{\text{pl}},$$

where ν is the Poisson's ratio, ε_r, ε_θ and ε_z are strains in principal directions σ_r, σ_θ, σ_z are stresses in principal directions, E is elastic modulus, ε^{th} is thermal strain, ε^s is strain due to swelling, ε^c is creep strain and ε^{pl} is plastic strain. Swelling and thermal strains are isotropic and hence $\varepsilon_r^{\text{th}} = \varepsilon_\theta^{\text{th}} = \varepsilon_z^{\text{th}} = \alpha T$ where α is linear thermal expansions coefficient and

$$\varepsilon_r^s = \varepsilon_\theta^s = \varepsilon_z^s = \tfrac{1}{3} \text{ (volumetric swelling).}$$

Creep and plastic strains are calculated using equivalent stress σ^* which is defined as

$$\sigma^* = \frac{1}{\sqrt{2}}[(\sigma_r - \sigma_\theta)^2 + (\sigma_\theta - \sigma_z)^2 + (\sigma_r - \sigma_z)^2]^{1/2}.$$

Though the constitutive equations remain the same, codes developed may differ in degree of details, numerical methods used and processes modelled.

The fuel modelling codes developed to describe the behaviour of nuclear fuel elements fall in two general groups. In the first category, the models are more phenomenological and consist of a fast-running, empirical models of processes to describe the fuel behaviour. In the second category of codes, the models are treated in more detail and include the various processes which are considered to control the behaviour of the fuel elements. The main objective of such codes is to relate the material properties and physical mechanism to the widest possible range of fuel element geometries, material parameters and operating conditions. Because of the firm physical basis for the models, these codes allow extrapolation over a wide range of conditions.

A number of codes have been developed for nuclear fuel elements all over the world. Some of the well known fuel modelling codes are COMETHE (Belgium), ELESIM (Canada), MINIPAT and SLEUTH SEER (UK), URANUS (FRG), LIFE (USA). In India two computer codes have been developed for analysis of water reactor fuel element performance, PROFESS (Sah and Venkatesh 1983, 1984) and COMTA (Anand *et al* 1980). PROFESS is used for analysis and interpretation of post-irradiation examination results obtained on fuel elements (Roy *et al* 1984).

6. Summary

A review of the important effects observed in metallic uranium and ceramic nuclear fuels during irradiation has been made. The mechanism of the processes occurring in the fuel during irradiation has been discussed. The basic cause of several effects in fuel

arises from the effects of highly ionised fission fragments and high energy neutrons. The fission fragments give rise to fission spike, lattice defects and impurity atoms in the fuel.

Alpha uranium exhibits dimensional instability during irradiation. This is caused by three irradiation-induced phenomena namely irradiation growth (shape change at constant volume without any external stress application), irradiation creep (deformation under small external stress) and swelling (due to solid and gaseous fission products). Irradiation growth of uranium is related to the anisotropy of alpha uranium crystal and the mechanism of growth involves formation of extra layers of interstitial atoms on certain crystallographic planes.

A very severe thermal and radiation environment (fuel temperatures approaching melting point and thermal gradients in the range 3000–5000°C/cm) initiates a number of interactive processes in the ceramic fuel during irradiation. Several spectacular changes in geometry, dimension, chemistry and microstructure of the fuel are observed. Shrinkage and dissolution of as-fabricated pores by fission fragments leads to fuel densification in the early stages of fuel irradiation. The initial microstructure of the fuel gets altered and several restructured radial zones are observed in fuel cross-sections. One of the important microstructural changes is the formation of high density columnar grain by movement of porosity towards the centre. Plutonium which is initially distributed uniformly in the fuel is observed to segregate to preferred locations (towards fuel centre or away from fuel centre) depending upon the initial stoichiometry of the fuel. Oxygen in the fuel gets redistributed to maintain the thermodynamic equilibrium between CO_2, CO and oxygen in the existing radial temperature gradient. Many fission products especially the noble metals and volatile elements produced in the fuel are also observed to redistribute themselves. A large fraction of fission products in fuel is the fission gases xenon and krypton which are insoluble in the fuel matrix. The fission gases precipitate as gas bubbles in the fuel and cause fuel swelling. A part of the fission gas is released from the fuel. The gas release occurs by three mechanisms: recoil and knock out (below 1000°C); atomic diffusion to the grain boundary (1000–1600°C) and bubble migration to the fuel centre (above 1600°C). Another important phenomena observed in ceramic fuel is irradiation creep. Irradiation-induced creep is found to take place in UO_2 at a low temperature (< 1100°C) where thermal creep is absent. Three types of mechanisms have been proposed: diffusion based, spike based and dislocation based. A satisfactory model of irradiation creep in ceramic fuel is yet to be developed.

References

Ainscough J B, Oldfield B W and Ware J O 1973–74 *J. Nucl. Mater.* **49** 117

Anand A K, Anantharaman K, Basu S and Mehta S K 1980 *Pellet cladding interaction in water reactors, Proc. IAEA Specialists Meeting, Risφ, Denmark*, IWGFPT 8, p. 31

Assman H and Stehle H 1978 *Nucl. Eng. Design* **48** 49

Assman H and Stehle H 1982 *Gmeling handbook of inorganic chemistry*, 8th edn. Uranium Suppl., Vol. A4, p. 114

Bahl J K, Sah D N, Chatterjee S and Sivaramakrishnan K S 1979 BARC Report, BARC-1014

Beiswenger H, Bober M and Schumacher G 1967 *Plutonium as a reactor fuel, Proc. Symp., Brussels*, p. 273

Bellamy R G and Rich J R 1969 *J. Nucl. Mater.* **33** 64

Bober M, Sari C and Schumacher G 1969 *Trans. Am. Nucl. Soc.* **12** 603

Bramman J I and Powell H J 1975 *J. Br. Nucl. Soc.* **1** 63

Brucklacher D 1975 *Physical metallurgy of reactor fuel elements* (London: The Metals Society) p. 118
Brucklacher D, Dienst W and Thummber F 1970 *Fast reactor fuel and fuel elements, Proc. Conf., Karlsruhe,* September
Buckley S N 1964 quoted by Robertson J A L 1969 in *Irriadation effects in fuels,* AEC Monogr. 1969 (New York: Gordon and Breach) p. 27
Chadderton L T and Torrens I M 1969 *Fission damage in crystals* (London: Methiren Co.)
Chubb W, Hott A C, Argall B M and Kilp G R 1975 *Nucl. Technol.* **26** 486
Chubb W 1972 *J. Nucl. Mater.* **44** 136
Collins D A, Hargreaves R and Hughes H 1973 *Nuclear fuel performance, Proc. BNES Conf.,* London, October, Paper 49
Cornell R M 1969 *Philos. Mag.* **19** 539
Cornell R M 1971 *J. Nucl. Mater.* **38** 319
Dienst W 1977 *J. Nucl. Mater.* **65** 24
Gilbert E R 1971 *Reactor Technol.* **14** 258
Gittus J H 1978 *Irradiation effects in crystalline solids* (Barking Appl. Sci. Pub.) chap. 3
Holden A N 1958 *Physical metallurgy of uranium* (Massachusetts: Addison Wesley) p. 38
Howe J P and Weber C E 1957 quoted by Robertson J A L 1969 in *Irradiation effects in nuclear fuels,* AEC Monogr. (New York: Gordon and Breach) p. 40
Konobeevsky S T, Pravdyuk N F and Kutaitsev V I 1955 *Proc. First Int. Conf. on Peaceful Uses of Atomic Energy,* (New York: UNO) Vol. 7, p. 443
Kopelman B 1959 *Materials for nuclear reactors* (New York: McGraw Hill) p. 227
Legget R D, Mastel B and Bierlein T K 1964 US Report HW-79559
McDonnel W R 1973 *Physical metallurgy of reactor fuel elements, Proc. Conf., Berkeley,* September, p. 266
Notley M J F and Hastings I J 1980 *Nucl. Eng. Design* **56** 163
Olander D R 1976 *Fundamental aspects of nuclear reactor fuel elements,* TID-26711, chapters 11, 14 and 16
Ostberg G 1965 Kjeller Report KR-89, p. 63
Paine S H, Kittel J H 1955 *Proc. I Int. Conf. on the Peaceful Uses of Atomic Energy* (New York: UNO) Vol. 7, p. 445
Pickman D O 1984 *Fuel element performance computer modelling, Proc. IAEA Specialists Meeting, Windermere, UK* (to be published)
Pugh S F 1955 *Proc. I Int. Conf. on the Peaceful Uses of Atomic Energy* (New York: UNO) Vol. 7, p. 441
Roberts A C and Cottrell A H 1956 *Philos. Mag.* **8** 711
Robertson J A L 1969 *Irradiation effects in nuclear fuels,* AEC Monogr. (New York: Gordon and Breach) pp. 27 and 45
Ross A M 1969 *J. Nucl. Mater.* **30** 134
Roy P R and Sah D N 1983 *Irradiation effects in solids, Proc. Symp., BARC* (to be published)
Roy P R, Purushotham D S C, Kamath H S and Sah D N 1984 Improved utilisation of water reactor fuels with special emphasis on extended burn-up and plutonium recycling, IAEA Specialists Meeting, CEN/SCK, Mol. Belgium
Sah D N and Venkatesh D 1983 *Irradiation effects in solids, Proc. Symp., BARC, Bombay* (to be published)
Sah D N and Venkatesh D 1984 *Water reactor fuel element performance computer modelling, Proc. IAEA Specialists Meeting, Windermere, UK* (to be published)
Solomon A A, Routbort J L and Voglewede J C 1971 Report ANL-7857
Turnbull J A and Cornell R M 1970 *J. Nucl. Mater.* **36** 161
Turnbull J A 1971 *J. Nucl. Mater.* **38** 203
Wapham A D 1966 *Nucl. Appl.* **2** 123